Journal of Metals, Materials and Minerals, 34(3), 1947, 2024

Use of commercial synthetic filament waste to reinforce biobased poly(butylene succinate) with the aid of compatibilizers

Nattakarn HONGSRIPHAN[1,*], and Alongkorn POPANNA[1]

[1] *Department of Materials Science and Engineering, Faculty of Engineering and Industrial Technology, Silpakorn University, Nakhon Pathom, 73000, Thailand*

***Corresponding author e-mail**: Hongsriphan_N@su.ac.th

Received date:
25 January 2024
Revised date:
22 April 2024
Accepted date:
3 July 2024

Keywords:
Poly(butylene succinate);
synthetic filament;
HMDI;
HMDA;
Short fiber reinforced composite

Abstract

Since poly(butylene succinate) (PBS) has low rigidity for engineering application, this research attempted to reinforce PBS with poly(ethylene terephthalate) (PET) and polyamide-6 (nylon6) filaments with the reservation of polymer toughness. Filaments were chopped to be short fibers (length of 2 mm to 4 mm) and melt compounded with PBS pellets in the weight ratio of 1 wt%, 5 wt%, and 7 wt% using a twin-screw extruder that the temperature profile was set high enough for melting only PBS matrix. Two types of compatibilizers; hexamethylene diisocyanate (HMDI) or hexamethylene diamine (HMDA) of 0.05 wt% were used to treat fiber surface. It was found that tensile modulus of PBS increased with respect to fiber concentration, which untreated PET fibers provided higher tensile modulus about 2% to 7%. Surface treatment of fibers with either HMDI or HMDA increased rigidity of the composites, while elongation at break and impact strength were also improved with respect to fiber concentration. Also, shifting in glass transition temperature of PBS by DMA indicated improved interfacial interaction, which HMDA treatment gave the best benefit for mechanical properties. Number-average molecular weight of HMDI-treated composites was closed to extruded PBS, however, those of HMDA-treated composites were reduced dramatically implying chain scission highly occurred. SEM micrographs revealed good interfacial adhesion obtained after fiber treatment. Crystallization of PBS studied by XRD showed that the crystal form was not affected by the compatibilizer.

1. Introduction

Poly(butylene succinate) (PBS) is an aliphatic polyester that has been increasing commercial interest due to its ability to be 100% renewable biomaterial with lower cost in the near future [1]. Its raw materials, butanediol and succinic acid, could be synthesized from bio-based renewable resource [2]. Currently, PBS is a petroleum-based biodegradable polymer that is synthesized by polycondensation of succinic acid with 1,4-butanediol. Depending on grades available in the market, it is typically a semi-crystalline polymer with a melting point of 112°C to 115°C, a density of 1.25 $g \cdot cm^{-3}$ to 1.26 $g \cdot cm^{-3}$, a heat deflection temperature of about 90°C, and mechanical properties similarly to low-density polyethylene (LDPE) or high-density polyethylene (HDPE). PBS has plenty desirable properties for marketing, including biodegradability, melt process ability, good crystallization, and can be dyed. The current application of PBS is mainly produced in packaging fields, such as food and cosmetic packaging; disposable products such as medical articles; and in agricultures, such as mulching films and delayed release materials for pesticide and fertilizer. Since LDPE is petroleum-based polymers which is widely used in flexible packaging, PBS could be used to replace LDPE for sustainable purpose [3]. Moreover, mechanical properties of PBS depend on the degree of crystallinity, which its chemical structure is based on polyester that is stronger than polyethylene.

With the continuing development of PBS with higher molecular weight or copolymerization route, it is expected to apply in the engineering application, such as plastic housing for electrical and electronic devices. Development of PBS in composite form has also been being conducted for automotive part [4]. It has been attracted to researchers attempting to improve mechanical strength of PBS by reinforcing with lignocellulosic fillers, such as sisal [5,6], basalt [7], coconut, sugarcane bagasse, curaua [8], ramie [9], cellulose nanocrystal [10]; as well as by reinforcing with inorganic fillers, such as calcium carbonate nanoparticle [11], nano-titanium dioxide [12], and carbon nanotubes [13]. Although tensile modulus and tensile strength of the PBS-based composites were enhanced with these reinforcements, the advantage of PBS being flexible polymer like LDPE was deteriorated. This could cause the PBS-based composites to withstand lower impact loading if the interfacial adhesion between PBS matrix and the reinforcing fillers is not good enough for load transfer.

Since there are plenty of synthetic filament (SF) waste from textile industries, they could be used to reinforce polymeric matrix to improve rigidity which preserves flexibility. According to Maurya *et al.* [14], they reviewed several researches that nylon fiber have been used as a reinforcing material in various polymeric matrix, such as polyethylene terephthalate, polymethyl-methacrylate, polycarbonate, and elastomer

materials. Abraham and George [15] compounded polypropylene (PP) with nylon6 fibers of three diameters at levels up to 30 wt%. They reported that the addition of nylon6-SFs improved mechanical properties, such as tensile strength and flexural strength. The least diameter fibers gave the maximum improvement in mechanical properties. They also enhanced interfacial adhesion between fibers and matrix by grafting PP matrix with maleic anhydride in the presence of styrene.

F. Ke *et al.* [16] prepared the binary PP/nano-$CaCO_3$, PP/PET-SF, and ternary PP/nano-$CaCO_3$/PET-SF composites by melt blending method, which they aimed to balance toughness and stiffness of the PP composites. Ethylene-butyl methacrylate-glycidyl methacrylate was added to improve compatibility among them. They reported that the glass transition temperature of PP matrix was increased and mechanical properties, especially the impact strength was significantly improved. The reinforcing mechanism was mainly due to the β-crystalline phase of PP induced by the synergistic effect of PET-SFs and nano-$CaCO_3$.

Lee and Wang [17] studied effect of lysine-based diisocyanate (LDI) as a coupling agent on properties of poly(lactic acid)/bamboo fiber composite and poly (butylene succinate)/bamboo fiber composite in the weight ratio of 70/30 wt%. The calculated N=C=O content was varied to be 0.11 wt% to 1.30 wt% of the composites. From SEM micrographs, both composites after compounding with LDI of 0.65% showed that bamboo fiber appeared to be coated with polymer matrix. The improved interfacial adhesion was due to the compatible effect of graft copolymer with LDI intermediates, which could be produced through a chemical reaction between the hydroxyl groups of polyester and bamboo fibers under melt kneading conditions. As a result, mechanical properties of the LDI-added polyester-based composites were increased.

Onyeagoro *et al.* [18] investigated effect of maleated polyisoprene (MAPI)/hexamethylene diamine (HMDA) dual compatibilizers and filler loading on physico-mechanical properties of natural rubber (NR)/poly(ethylene terephthalate) (PET)/dikanut shell powder composites, which NR/PET composition was fixed at 60/40 wt%, and the filler loadings was varied 0 wt% to 8 wt%. They reported that addition of a small amount of HMDA could act as an effective coupling agent to produce PET-co-HMDA-co-MAPI copolymers at the interface. The better physico-mechanical and water uptake propertie of the composites was attributed to the improved compatibility that the composites had finer domain size of the dispersed phase with greater interfacial adhesion.

In our previous work [19], the commercial nylon6-SFs without any chemical treatment was used to enhance mechanical properties of PBS. It was found that higher fiber concentration increased tensile modulus and impact strength of the composites but decreased tensile strength. From DSC results, it showed that nylon6-SFs acted as nucleating agent for PBS molecules to crystallize faster. However, the degree of crystallinity was reduced compared to PBS. Also, adding nylon6 fibers did not affect thermal stability of PBS as seen in TGA results under oxygen atmosphere.

The benefit to use synthetic fibers (SFs) to reinforce PBS matrix has been pursued with the aim of improved interfacial adhesion between them. In this research, two types of commercial polymeric filaments; PET and nylon6, were chopped to be short fibers and compounded into PBS in the concentration of 1 wt%, 5 wt%, and 7 wt% to produce the SF-reinforced composites. These commercial synthetic filaments are widely used in various applications, and could be disposed in both the industrial and municipal waste. Hexamethylene diisocyanate (HMDI) and hexamethylene diamine (HMDA) were used to treat surface of SFs prior to the melt compounding. Mechanical properties of the SF-reinforced composites by means of tensile and impact testing were evaluated and compared. Thermo-mechanical properties and improved compatibility between polymer matrix and SFs were investigated using dynamic mechanical analysis (DMA). Change of number-average molecular weight of PBS in the SF-reinforced composites was determined using intrinsic viscosity method. Morphology of the SF-reinforced composites was characterized using scanning electron microscopy (SEM). Finally, crystallization of PBS matrix in the presence of SFs was also studied via differential scanning calorimetry (DSC) and X-ray diffraction (XRD).

2. Experimental

2.1 Materials

PBS (GS Pla®, Grade FZ91PD) was purchased from Mitsubishi Chemicals, Japan, which had a melt flow index (MFI) of 5 g/10 min (at 190°C, 2.16 kg), a density of 1.26 g·cm^{-3} and a melting temperature of 115°C. Polyethylene terephthalate (PET) and polyamide6 (nylon6) filaments, were supplied by Thai Toray Synthetics Co. Ltd, Thailand. These synthetic filaments (SF) were commercially used to produce clothing and mattress.

Figure 1 shows SEM micrographs of these filaments, which the diameter of PET filament was about 41 μm and that of nylon6 filament was about 26 μm. Table 1 shows tensile modulus and tensile strength of PET and nylon6 filament, which were determined according to ASTM-D3822 and supplied by the filament supplier. According to the data, PET filament is more rigid than nylon6 filament but has lower tensile strength.

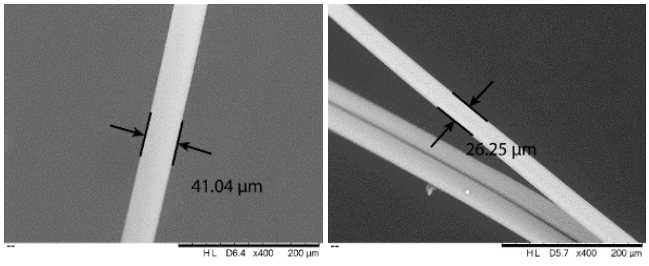

Figure 1. SEM micrographs (magnification of 400×) of PET (left) and nylon6 filaments (right).

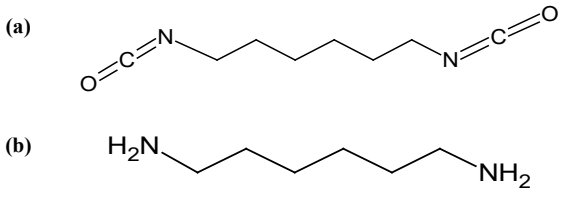

Figure 2. Chemical structures of (a) HMDI and (b) HMDA.

Table 1. Tensile modulus and tensile strength of synthetic filaments (SF).

SF	Tensile modulus (MPa)	Tensile strength (MPa)
PET	2,250 ± 89	153 ± 13
nylon6	1,248 ± 93	278 ± 23

Table 2. Abbreviations and compositions of PBS/SF composites.

Sample	PBS (wt%)	Fiber concentration (wt%)	HMDI or HMDA (wt%)
PBS	100.00	0.00	0.00
PBS_SF1 untreated	99.00	1.00	0.00
PBS_SF5 untreated	97.00	3.00	0.00
PBS_SF7 untreated	95.00	5.00	0.00
PBS_SF1 treated	98.95	1.00	0.05
PBS_SF5 treated	96.85	3.00	0.15
PBS_SF treated	94.75	5.00	0.25

Two types of compatibilizers; hexa-methylene diisocyanate (HMDI, purity > 98%) and hexamethylenediamine (HMDA, purity > 97.5%), were purchased from Sigma-Aldrich Co LLC. Their chemical structures are presented in Figure 2. Acetone and deionized water were also used to dissolve compatibilizers for fiber treatment.

2.2 Fiber preparation

PET and nylon6 synthetic filaments (PET-SFs or nylon6-SFs) were chopped to a length of 2 mm to 4 mm, washed thoroughly with ethanol for 10 min and rinsed with acetone to remove oil or any contamination. Washed SF fibers were dried in an air-circulating oven at 60°C for 12 h prior compounding. For fiber treatment, washed/dried SF fibers were sprayed with a solution of HMDI (in acetone) or HMDA (in ionized water) and dried at 60°C for 12 h. A concentration of each compatibilizer was kept constant at 0.05 wt% of dried SF weight.

2.3 Melt compounding and fabrication

Before compounding, PBS pellets were dried in an air-circulating oven at 60°C for 12 h. PBS pellets and dried PET-SFs or nylon6-SFs were compounded using the fiber concentration of 0 wt%, 1 wt%, 5 wt%, and 7 wt% of the composites. The compounding was carried out in a co-rotating twin-screw extruder (SHJ-25, Yongteng, China) with a screw speed of 60 rpm and the temperature profile of 118-125-130-140-140-140-140-140°C. Extrudates were water-cooled, pelletized, and dried immediately in an oven at 60°C for 12 h.

Table 2 presents sample abbre-viations and compositions of PBS/SF composites prepared in this study. PBS pellets with no fibers were also extruded and fabricated under the same thermal history which was designated as PBS. Dogbone-shape and rectangular specimens were fabricated by injection molding (Battenfeld, BA250CDC, England) using the nozzle temperature of 120°C and the mold temperature of about 30°C.

2.4 Characterization and testing

Tensile testing was performed in accordance to ASTM-D638 using a universal testing machine (Instron 5969, Instron Engineering Corporation, USA). The testing was carried out using a crosshead speed of 10 mm·min^{-1}. Ten specimens were tested which the averages and deviations of tensile modulus, ultimate tensile strength, and elongation at break were calculated and evaluated.

Notched Izod impact testing was performed in accordance to ASTM-D256 using an impact tester (Zwick, B5102.202, Germany) with a pendulum hammer of 4.0 J. Ten specimens were tested which the average and its deviation of impact strength were calculated and evaluated.

Thermal properties of PBS and PBS/SF composites were evaluated using a differential scanning calorimeter (DSC1, Mettler-Toledo, Switzerland). Samples were tested in a heat-cool-heat mode and heated from 30°C to 140°C at a heating rate of 10°C·min^{-1}. Melting temperatures (T_m) and crystallization temperature (T_c) were determined from thermogram and reported. The degree of crystallinity (X_c) was calculated as the following Equation (1):

$$\%x_c = \frac{\Delta H_m}{\Delta H_m^o} \times \frac{100}{w} \quad (1)$$

where ΔH_m was melting enthalpy of crystallinity (J·g^{-1}), ΔH_m^o was melting enthalpy of 100% crystalline of PBS (110.3 J·g^{-1}) [20], and w was weight fraction of PBS in the composites.

Dynamic mechanical analysis (DMA) of PBS and PBS/SF composites was carried out with a dynamic mechanical analyzer (GABO Qualimeter/EPLEXOR QC 25, Germany). The analysis was performed between –60°C and 80°C at a heating rate of 2°C·min^{-1}. The experiment was done in a tension mode with a frequency of 10 Hz, a static strain of 0.1%, and a dynamic strain of 0.05%.

Number-average molecular weight (M_n) of the PBS matrix was evaluated following the method described by Tianxiang Jin *et al.* [21]. For each composite sample, it was dissolved in Chloroform and fibers were filtered out. Sample solution was prepared with a concentration of 0.4 g·cm^{-3} and determined their Intrinsic viscosities (IV) using an Ubbelohde viscometer at 25°C. The Intrinsic viscosities and M_n were calculated by the following Equations (2-3):

$$[\eta] = \frac{\left\{2\left(\frac{t}{t_0} - \ln\left(\frac{t}{t_0}\right) - 1\right)\right\}^{1/2}}{c} \quad (2)$$

$$M_n = 3.29 \times 10^4 [\eta]^{1.54} \quad (3)$$

where c was the concentration of the solution, t was the flow time of sample solution, t_0 was the flow time of pure solvent (Chloroform), [η] was the intrinsic viscosity, and M_n was the number-average molecular weights. M_n of extruded PBS was evaluated and defined as PBS, and M_n of as-received PBS pellets was also evaluated and defined as pure PBS.

Morphology was examined by a scanning electron microscope (SEM) (TM-3030, Hitachi, Japan). The cryofracture fractured surface and the tension fractured surface was platinum/gold coated prior to inspection to avoid electrostatic charging before examination. For cryo-fractured surface, the tensile specimens were soaked in liquid nitrogen and then were broken by a hammer. For tension-fractured surface, the broken specimens after tensile failure were selected for examination.

X-ray diffraction of PBS and PBS/SF composites was evaluated using an X-ray diffractomer (Miniflex 2, Rigaku, Japan). Samples were tested under a WXRD mode with a wavelength (Cu-Kα) of 1.531841 A°, and was scanned within the range of 0° to 50° (2θ).

3. Results and discussion

3.1 Mechanical properties of PBS and PBS/SF composites

Since both PET and nylon6 polymers have higher tensile modulus than PBS polymer as shown in Table 1, blending them into PBS matrix is expected to improve rigidity of the blends although these polymers are blended at the processing temperature that they are still in the fiber form. This kind of blending is similar to using aramid (aromatic polyamide) fibers to reinforce thermo-setting resin such as epoxy or polyester resins. Tensile moduli of PBS and PBS/SF composites are presented in Figure 3. It is clearly seen that these short fibers increased tensile modulus with respect to fiber concentration. This agreed with the study by Asgari and Masoomi [22]. However, they reported that at low fiber concentration such as 5 wt% or 10 wt% short fiber the applied stresses to the composites were not properly distributed for polypropylene/PET-SF composites. As observed later in SEM micrographs, the proper interfacial interaction among the PBS matrix and PET-SFs untreated or nylon6-SFs untreated still provided the fairly load transfer implying there was secondary interaction within the elastic deformation range. Blending PET-SFs into the PBS matrix yielded higher tensile modulus than those blending nylon6-SFs. This was basically due to the PET filament had higher modulus than nylon6 filament as reported in Table 1. After surface treatment with HMDA, it was seen that tensile modulus of the PBS composites was significantly improved, especially in the composites adding PET-SFs. HMDI treatment on fibers showed marginal effect to increase tensile modulus. This was due to the different improved compatibility between the PBS and the treated SFs, which confirmed by the shifting of glass transition temperature that was evaluated by the DMA.

Table 3 presents the measured tensile modulus of the PBS/SF composites, which the theoretical tensile modulus was calculated from the rule of mixture (ROM) as a benchmark using the following Equation (4).

$$E_c = E_m w_m + E_r w_r \quad (4)$$

where E_c was theoretical tensile modulus of the composites, E_m was measured tensile modulus of the PBS matrix, E_r was measured tensile modulus of fiber reinforcement (shown in Table 1), w_m was weight fraction of PBS matrix in percentage, and w_r was weight fraction of fiber reinforcement in percentage.

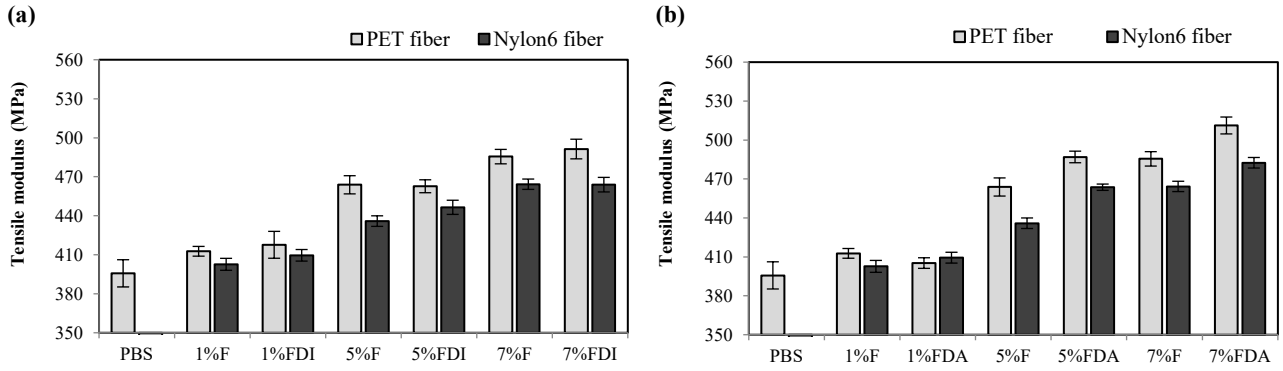

Figure 3. Tensile modulus of PBS, PBS/SF untreated composites, and PBS/SF composites treated with (a) HMDI or (b) HMDA.

Table 3. Measured tensile modulus and theoretical tensile modulus from the rule of mixture.

SF concentration (wt%)	E_{PET} (MPA) calculated from the rule of mixture	E_{PET} (MPA)	$E_{PET, HMDI}$ (MPA)	$E_{PET, HMDA}$ (MPA)	E_{nylon6} (MPA) calculated from the rule of mixture	E_{nylon6} (MPA)	$E_{nylon6, HMDI}$ (MPA)	$E_{nylon6, HMDA}$ (MPA)
0	396	396	396	396	396	396	396	396
1	415	412	418	405	405	403	409	409
5	489	464	463	487	439	436	446	464
7	526	485	491	511	456	464	464	482

It was found that theoretical tensile modulus of the PBS/SF composites adding nylon6-SF untreated was almost identical with the measured tensile data, while the composites adding PET-SFs untreated had lower the measured modulus than the theoretical modulus when the concentration was higher than 1 wt%. After treatment PET-SFs with HMDI or HMDA, tensile modulus of the composites was increased but still lower than the theoretical tensile data. It should be noted that the treatment of nylon6-SFs with HMDA enhanced tensile modulus of the PBS/SF composites to be significantly higher than the theoretical tensile data calculated from the rule of mixture. This emphasized the influence of chemical interaction between PBS polyester matrix and nylon6-SFs, which the compatibility improvement was evaluated by the DMA

Figure 4 presents the stress-strain curves of the composites added the highest fiber concentration in the research. Every curve presented ductility behavior resemble to that of PBS. It was clearly seen that adding short polymeric fibers enhanced rigidity of the PBS matrix with the benefit of higher extension, which compatibilizers provided greater toughness into composites. This was in contrast with the polymeric composites reinforced with lignocellulosic fibers, which the rigidity was improved in the expense of toughness reduction of the polymeric matrix. Figure 5 and Figure 6 show ultimate tensile strength and elongation at break of PBS and PBS/SF composites, respectively. The ultimate tensile strength of these PBS-based composites occurred at break. It is well known for researchers that the fiber matrix interface is the critical factor at which localized stresses are usually the highest at or near the interface which would become the point of premature failure of the composite. Hence, treated SF composites usually have the significant greater ultimate tensile strength. In contrast to tensile modulus, it is seen that using HMDI to treat the polymeric fibers enhanced tensile strength of the PBS/SF composites to be much greater than using HMDA. This is attributed to the reduction of molecular weight of PBS matrix as studied by the determination of M_n.

Since these fibers were crinkled and bended as observed in SEM micrographs, enough interfacial adhesion between matrix and fibers allowed composites to be extended longer while transferring the load from the main matrix to the fiber reinforcement. In both untreated and treated SF composites, elongation at break of PBS/nylon6-SF composites were higher than that of PBS/PET-SF composites which correlated with the improvement of interfacial adhesion of the nylon6-SFs. However, there was not noteworthy difference in the enhancement provided by treating the polymeric SFs with HMDI and HMDA in terms of elongation at break.

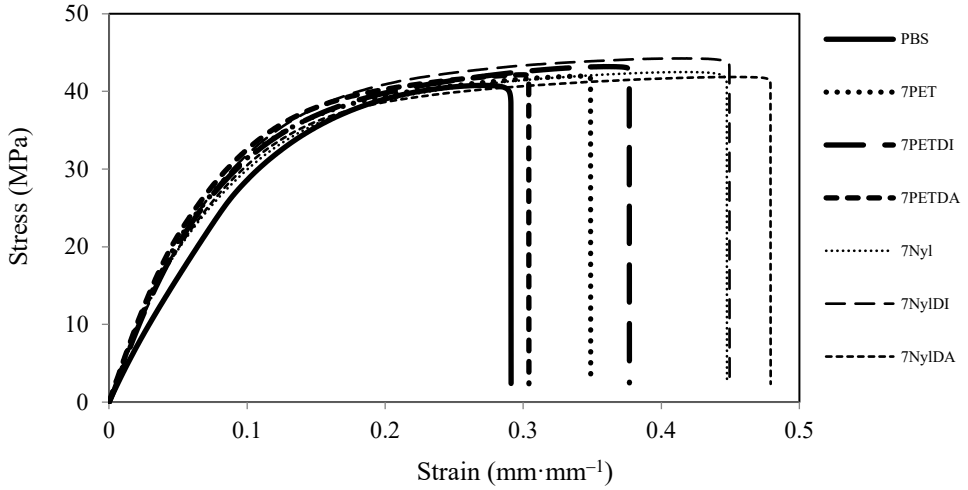

Figure 4. Stress-strain curves of PBS, PBS/PET-SF, and PBS/nylon6-SF composites, which the fibers were untreated, HMDI-treated or HMDA-treated fibers. The fiber concentration was 7 wt% in all the composites.

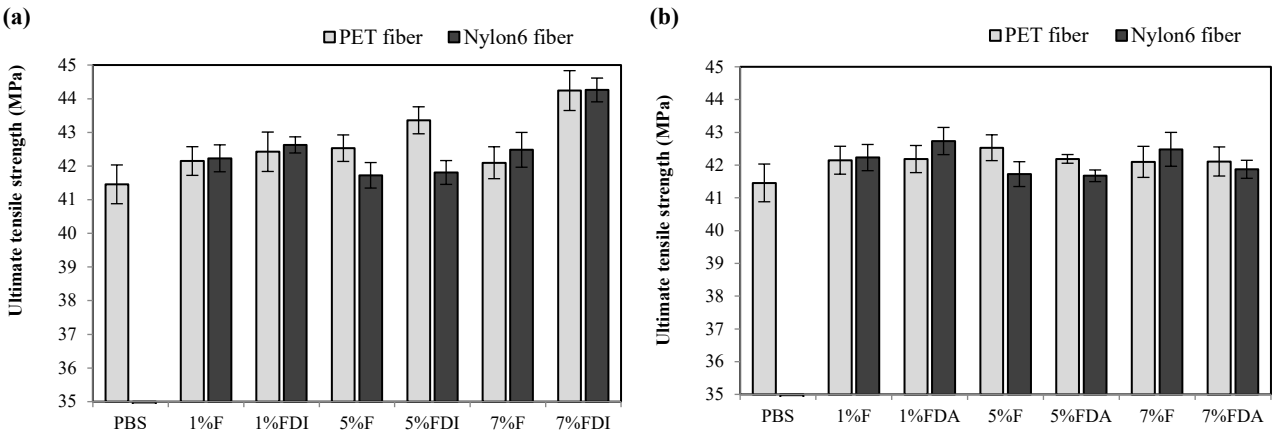

Figure 5. Ultimate tensile strength of PBS, PBS/SF untreated composites, and PBS/SF composites treated with (a) HMDI or (b) HMDA.

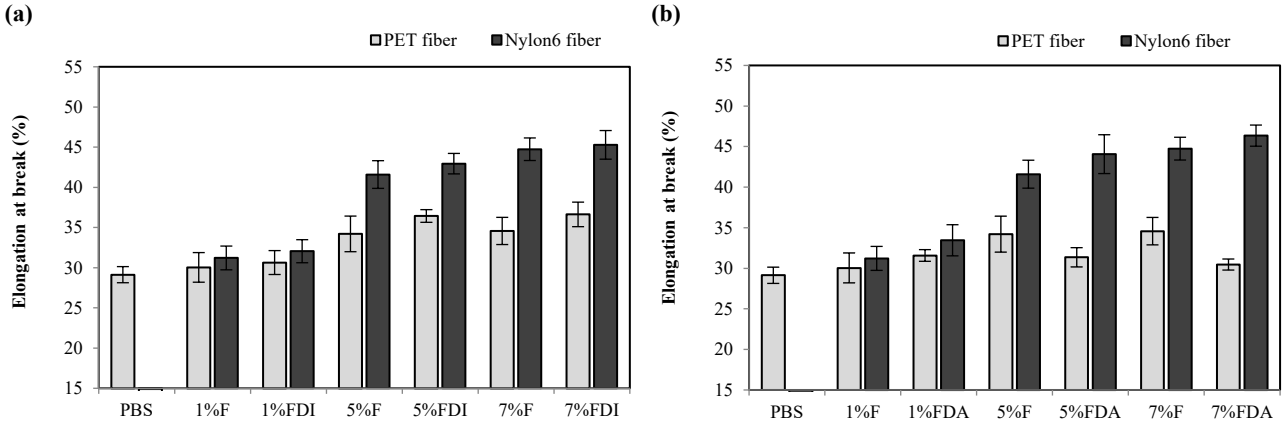

Figure 6. Elongation at break of PBS, PBS/SF untreated composites, and PBS/SF composites treated with (a) HMDI or (b) HMDA.

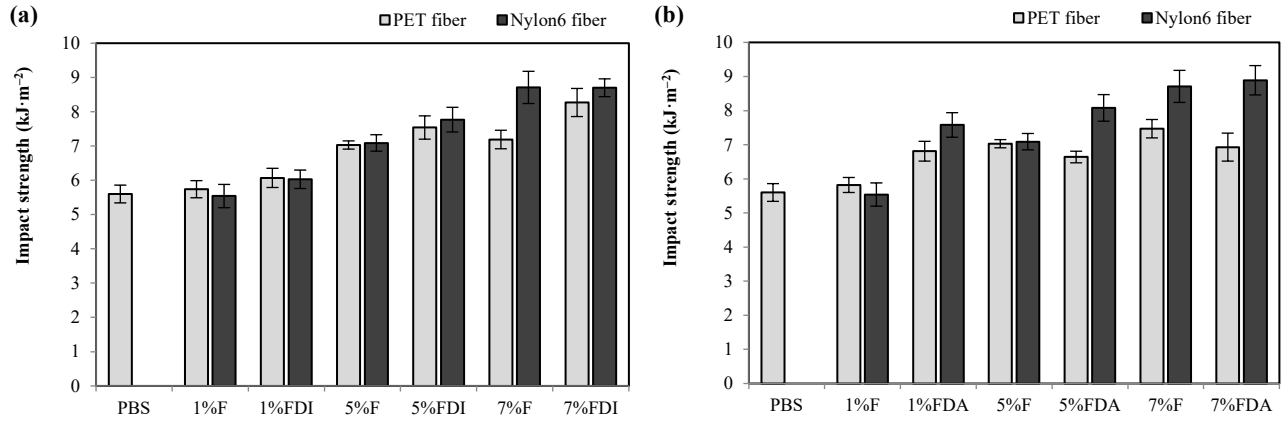

Figure 7. Impact strength of PBS, PBS/SF untreated composites, and PBS/SF composites treated with (a) HMDI or (b) HMDA.

Toughness of PBS and their PBS/SF composites is also evaluated in terms of notched Izod impact strength which the results are shown in Figure 7. It is observed from the figures that the PBS/PET-SF composites and PBS/nylon6-SF composites had significant higher impact strength compared to that of PBS. In contrast with tensile modulus, adding nylon6-SFs improved impact strength of the PBS matrix better than adding PET-SFs. This would be attributed to two factors; the fiber volume and the interfacial adhesion via secondary interaction. Since nylon6-SFs had smaller diameter, the fiber volume of the nylon6-SFs was higher for the same fiber concentration. Along with the achievable interfacial adhesion as evident in SEM micrograph, the impact energy could be dissipated in the PBS matrix yielding the higher impact strength with higher fiber concentration for the PBS/nylon6-SF composites. After these SFs were treated with HMDA, adding PET-SFs or nylon6-SFs of just 1 wt% concentration enhanced impact strength of PBS composites by 21% or 35%, respectively. It was found that HMDA enhanced the toughness of the PBS/nylon6-SF composites while toughness of the PBS/ PET-SF composites was better improved by using HMDI.

3.2 Thermal properties of PBS and the PBS/SF blends

Since the semi-crystalline PBS is a biodegradable polyester, mechanical properties as well as biodegradability depend on the degree of crystallinity (X_c). It is well known that the water absorption can be prohibited or delayed in the hydrophilic semi-crystalline polymer with the high X_c. Moreover, adding fillers into the semi-crystalline polymer would act as nucleate agents to obtain higher X_c. From DSC analysis, melting and crystallization temperatures of PBS and PBS/SF composites are summarized in Table 4.

It is seen that adding SFs showed clearly influence on the crystallization behaviour of PBS molecules when the fiber concentration was high or the fiber surface was chemical modified. Compared to PBS, the onset crystallization temperatures of both PBS/PET-SF and PBS/nylon6-SF composites were shifted to lower temperature, which the shifting of crystallization temperature in the PBS/nyon6-SF composites were more pronounced. This implied that the presence of these SFs interfered the nucleation of the PBS crystals. Bin Tan *et al.* [23] studied the crystallization behavior of PBS reinforced with cotton stalk bast fibers (CSBF) composites by DSC, which they discussed that the presence of cellulosic fibers promoted the nucleation of PBS molecules (polyester) while these fibers retarded the transport of polymer molecules resulting in a decreased crystallization rate. This implies that these SFs did not nucleate the PBS crystal onto their surface, and they inhibited the mobility of PBS molecules for crystallization.

Table 4. Crystallization temperatures (cooling scan) and crystal melting temperatures (2nd heating scan) of PBS and PBS/SF composites.

Sample	Crystallization temperature (T_c) (°C)		Crystal melting temperature (T_m) (°C)
	Onset	Peak	Peak
PBS	92.52	88.96	117.10
PET-SF untreated 1 wt%	92.29	88.81	116.58
PET-SF HMDI treated 1 wt%	92.39	88.80	117.26
PET-SF HMDA treated 1 wt%	92.35	89.32	115.29
PET-SF untreated 5 wt%	91.89	88.39	116.11
PET-SF HMDI treated 5 wt%	91.23	86.25	118.53
PET-SF HMDA treated 5 wt%	90.66	87.18	114.62
PET-SF untreated 7 wt%	90.95	86.08	118.21
PET-SF HMDI treated 7 wt%	91.86	87.39	116.09
PET-SF HMDA treated 7 wt%	90.57	86.53	114.74
Nylon6-SF untreated 1 wt%	91.65	87.48	118.19
Nylon6-SF HMDI treated 1 wt%	91.57	87.73	117.12
Nylon6-SF HMDA treated 1 wt%	92.18	88.22	117.78
Nylon6-SF untreated 5 wt%	91.22	86.83	116.78
Nylon6-SF HMDI treated 5 wt%	91.32	86.22	118.85
Nylon6-SF HMDA treated 5 wt%	91.50	87.04	116.40
Nylon6-SF untreated 7 wt%	90.23	84.12	119.24
Nylon6-SF HMDI treated 7 wt%	91.96	87.51	117.97
Nylon6-SF HMDA treated 7 wt%	90.32	85.87	117.58

Table 5. Glass transition temperatures (T_g) of PBS and PBS/SF composites by DMA.

Sample	PBS	Untreated PET-SF 7 wt%	HMDI-treated PET-SF 7 wt%	HMDA-treated PET-SF 7 wt%	Untreated nylon6-SF 7 wt%	HMDI-treated nylon6-SF 7 wt%	HMDA-treated nylon6-SF 7 wt%
T_g (°C)	-20.2	-17.9	-17.8	-17.4	-18.9	-17.6	-15.3

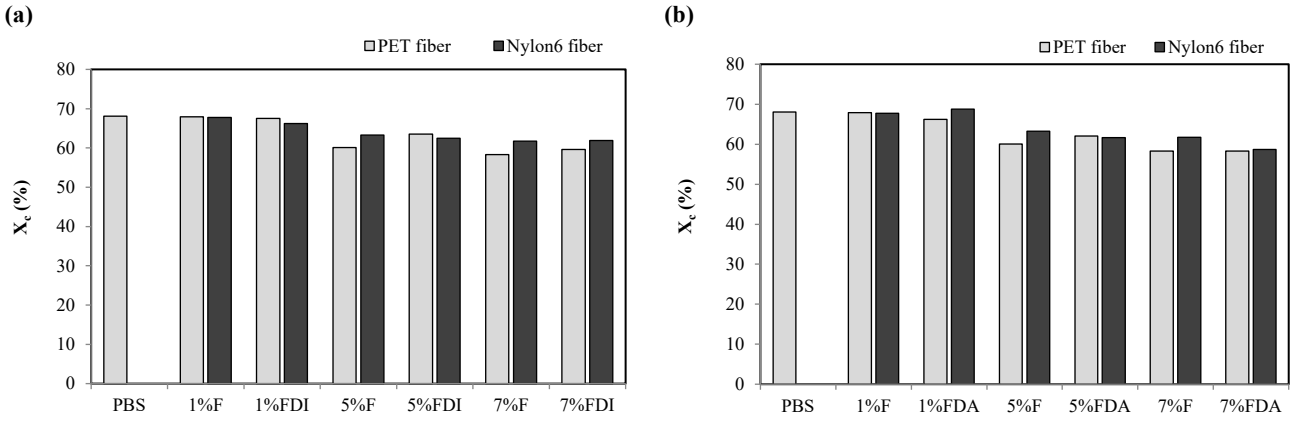

Figure 8. The degree of crystallinity (Xc) of PBS, PBS/SF untreated composites, and PBS/SF composites treated with (a) HMDI or (b) HMDA (the 2nd heating scan).

Considering the crystal melting temperature (T_m), it is seen that the T_m of the PBS matrix was shifted toward lower temperature when incorporating with PET-SFs. This implies the imperfection of the small crystal size of the PBS crystals. In contrast, the T_m of PBS matrix was shifted slightly toward higher temperature when incorporating with nylon6-SFs.

Figure 8 presents the X_c of PBS, PBS/SF composites, and PBS/SF composites with HMDI or HMDA as the compatibilizer. Observing the trends, it was clearly seen that the X_c decreased with the higher SF concentration, however, the composites reinforced with nylon6-SF had the higher X_c than those reinforced with PET-SFs. This is related directly to the M_n reduction of PBS matrix, so these relatively lower-M_n PBS molecules are more mobile to crystallize although these SFs are the barrier for the crystallization as evident in the decreased T_c

3.3 Dynamic mechanical properties of PBS and PBS/SF composites

Since the prepared composites consisted of the polymeric matrix and the reinforcing fibers with chemical treatment on fiber surface,

the thermo-mechanical properties of the composites were investigated using a dynamic mechanical analyzer in order to understand their viscoelastic properties. Figure 9 presents storage modulus and tan δ of PBS and the PBS/SF composites adding the fiber concentration of 7 wt%, which the glass transition temperatures (T_g) are summarized in Table 5. It is clearly seen that these SFs reinforced the PBS matrix to have higher storage modulus, and the treatment with HMDI or HMDA onto the SFs further improved the storage modulus of the composites. Similarly to tensile testing, the PBS/PET-SF untreated composite had higher storage modulus than the PBS/nylon6-SF untreated composite.

It is interesting to observe the influence of reinforcement before and after the glass transition of the PBS matrix. After the glass transition, the storage modulus of the PBS/nylon6-SF HMDI-treated or HMDA-treated composites did not differ significantly from the PBS/nylon6-SF untreated composite. Meanwhile, the storage modulus of the PBS/PET-SF composites was still in the same trend before and after the glass transition of PBS showing the improvement of storage modulus due to the fiber reinforcement. This related to the glass transition of these SFs themselves, which PET-SFs had the T_g about 80°C while nylon6-SFs had the T_g about 47°C. Unlike the PBS reinforced with lignocellulosic fibers [24], these polymeric fibers lose some rigidity (glassy state) if the surrounding temperature is higher than its glass transition temperature, and become more flexibility (rubbery state) to dissipate applied energy which is important for the impact loading.

From Table 5, it is seen that the T_g of PBS (or extruded PBS) was about –20.2°C and it was shifted to higher temperature for the PBS/SF composites. According to the determining of M_n, it was found that M_n of extruded PBS was either not changed (untreated or HMDI-treated) or reduced (HMDA-treated), the shifting of T_g to higher temperature indicated the chemical interaction between the PBS matrix and the SFs. Considering from the shifting of T_g, the secondary interaction (i.e. dipole-dipole interaction) between the untreated PET-SFs (–O–C=O–) and the PBS (–O–C=O–) was better than that between the untreated nylon6-SFs (–O–N=H) and the PBS (–O–C=O–). Treatment the PET-SFs with HMDI or HMDA did not have significant impact on the chemical compatibility since the T_g was not shifted significantly. In contrast, the treatment of the nylon6-SFs with HMDA could shift the T_g of PBS to occur at the higher temperature. This correlated to the M_n reduction of PBS in the HMDA-treated composite prompting the increasing carboxylic end groups of the depolymerized PBS to form secondary bonding (i.e. H-bonding) better with the active sites on the nylon6-SFs, which SEM micrograph reveals the wetting of PBS matrix onto the SFs that was extended to be observed as fibrillation during the tensile testing.

3.4 Impact of compatibilizer treatment on molecular weight of PBS matrix

In order to understand the role of compatibilizers to enhance mechanical properties of the PBS/SF composites, the number-average molecular weight (M_n) of PBS matrix was determined and compared with pure PBS (as-received PBS pellets). Figure 10 presents the M_n of pure PBS, PBS, PBS/PET-SF composites, and PBS/nylon6-SF composites.

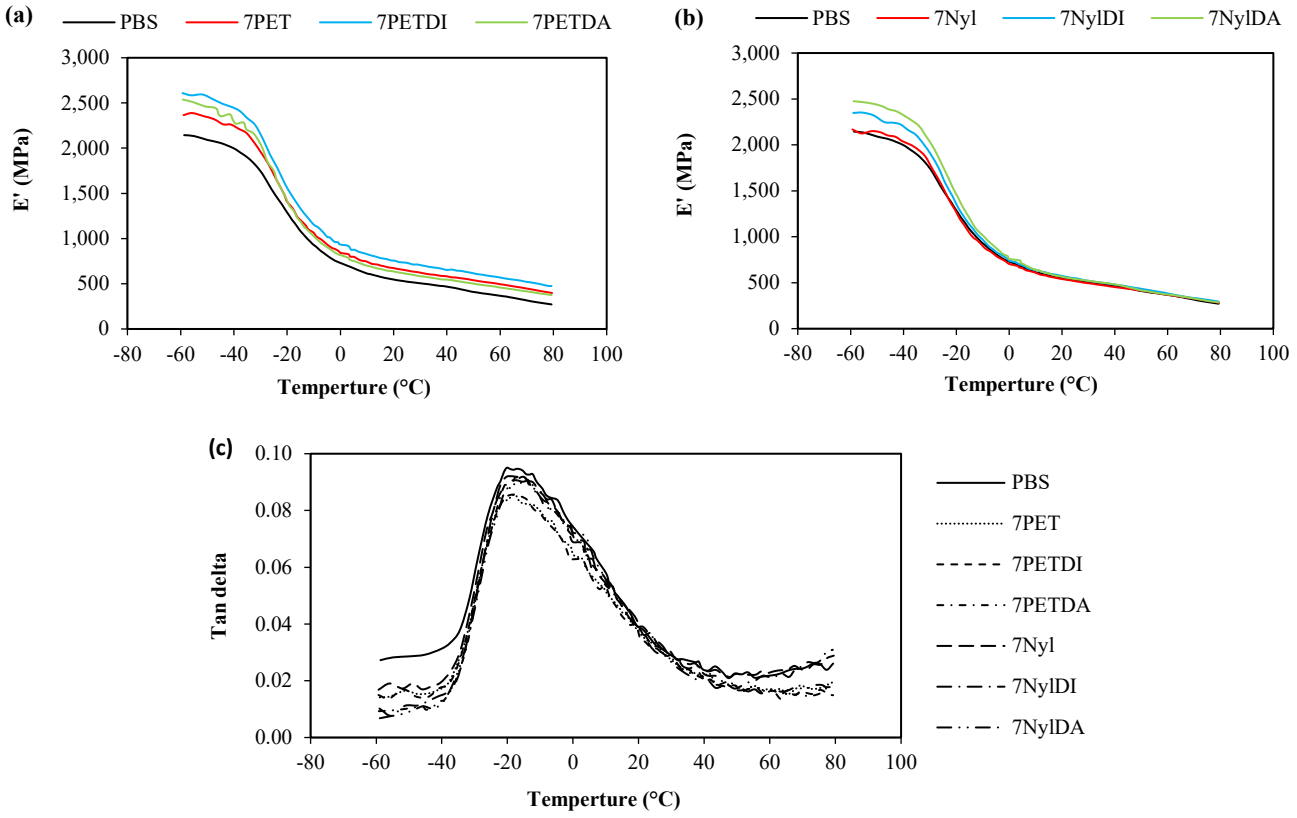

Figure 9. (a) Storage modulus (E′) of the PBS/PET-SF composites, (b) storage modulus of the PBS/nylon6-SF composites, and (c) tan delta of the PBS/SF composites compared with PBS.

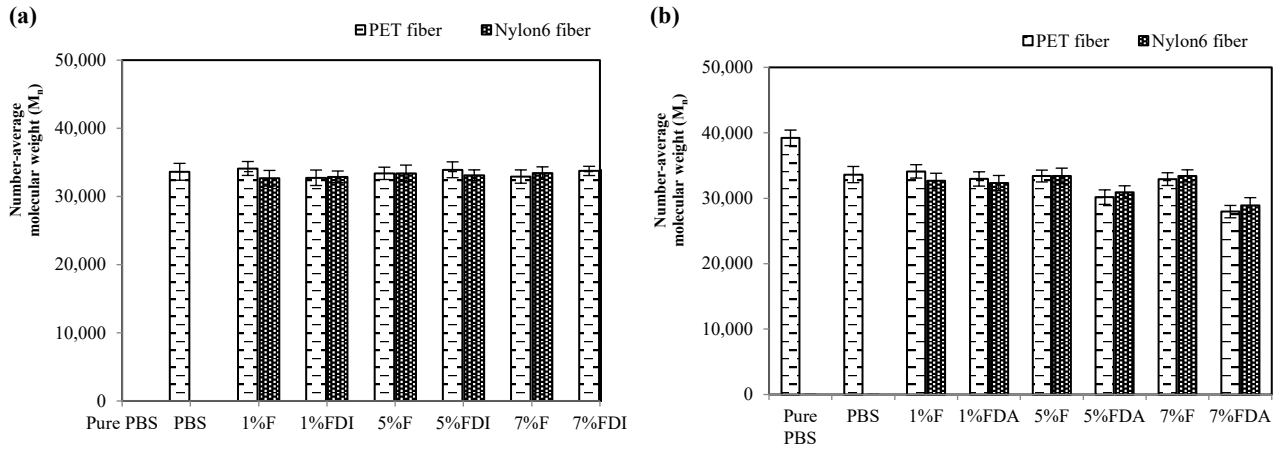

Figure 10. Number-average molecular weights of pure PBS, PBS, PBS/SF untreated composites, and PBS/SF composites treated with (a) HMDI or (b) HMDA.

It was found that M_n of PBS was reduced significantly after melt compounding and fabrication under high pressure. From the study of Rizzarelli and Carroccio [25], the commercial PBS would degrade under thermo-oxidative mecha-nism at temperature higher than 170°C, which the PBS backbone was ruptured related to the occurrence of α-hydrogen chain scission, followed by hydroperoxyl-dation. The initial step starts with a hydrogen abstraction from the methylene group adjacent to the ester linkage, leading to the formation of a hydroperoxide intermediate. Then, the unstable hydro-peroxide intermediates further undergo reaction with elimination of a hydroxyl radical. The radical formed can subtract a hydrogen radical from the bulk leading to the formation of the hydroxyl ester. The rearrangement reactions then proceed via the hydroxyl ester and produce oligomers bearing succinic acid, 4-hydroxy butanoic aldehyde or/and acid end groups.

Compared to PBS, compounding PBS with either untreated PET-SFs or untreated nylon6-SFs did not have effect on the M_n reduction significantly although there was the shifting in the glass transition temperature (T_g) slightly in the DMA results. Since the processing temperature did not melt these fibers, the compatibility between the PBS matrix and the untreated SFs was proposed to arise from H-bonding between the increasing carboxylic end groups of chain-scission PBS molecules and the active sites ($–NH_2$ or –OH groups) on the hydrophilic fiber surface.

Using HMDI as a compatibilizer in the melt compounding did not have impact on the M_n of PBS matrix. According to Raffa *et al.* [26], it is possible that diisocyanate in HMDI reacts with the hydroxyl end groups of PBS molecules leading to the formation of stable carbamate (or urethane), and/or reacts with the carboxylic end groups of the PBS molecules resulting branching on the PBS molecules that maintained the M_n of the thermo-degraded PBS. In this paper, the authors presume that diisocyanate (a fixed concentration HMDI of 0.05 wt% dried fibers) coated on the SFs would interact with hydroxyl end groups of the PET-SFs or carboxylic end groups of the nylon6-SFs, and then reacted with the carboxylic end groups of thermo-degraded PBS molecules during the reactive melt blending for improved compatibility as evident in the DMA analysis.

In contrast, using HMDA as a compatibilizer reduced the M_n of PBS with respect to the fiber concentrations. It is well known that PET polyester could be chemical depolymerized via aminolysis with diamine [27-29], such as hydrazine, benzylamine, ethylene-diamine, methy-lamine, ethylamine, ethanolamine, and hexamethylenediamine (HMDA). We proposed that PBS molecules reacted with HMDA via aminolysis resulting in the significant M_n reduction. Therefore, the reduction in melt viscosity due to the M_n reduction provided the better wettability of the PBS matrix onto the PET-SF or the nylon6-SF. Also, fibrillation of PBS matrix was observed from SEM micrographs in the tensile fractured specimens confirming good adhesion at the matrix-fiber interface.

3.5 Morphology of PBS and PBS/SF composites

Figure 11 shows SEM micrographs of as-received fibers and processed fibers in embedded in the PBS matrix. They reveal that PET-SFs and nylon6-SFs in the composites were intact in fiber form due to the processing temperature below the melting temperature of these SFs. However, the cross-section of PET-SFs was distorted slightly (Figure 11(a-b) from the original circular shape indicating the polymeric relaxation took place to release the residual stress induced from the fiber spinning process. This was due to the setting processing temperature was higher than the glass transition temperature (T_g) of these SFs. It is observed that the interface of SFs was closely adhered to the PBS matrix, however, some voids around the fibers as well as some fiber pullouts were also present. Voids around the SFs might result from the shrinkage of the SFs when they were surrounded with PBS melt, swelled and then cooled down. Moreover, the fiber breakage at the cryo-fractured surface was observed indicating that the interfacial adhesion via secondary interaction was established well enough for the untreated fibers themselves be broken rather than be pulled out.

Figure 12 presents SEM micro-graphs of tension-fractured surfaces of the PBS/PET-SF or PBS/nylon6-SF specimens after tensile testing. All specimens showed rough surface revealing ductile failure of PBS matrix during tensile testing. It was seen that PET-SFs and nylon6-SFs were embedded inside the PBS matrix in the random distribution arrangement. For the untreated composites in Figure 12(a) and Figure 12(d), the non-break fibers were pulled out from the PBS matrix which the PET-SFs (Figure 12(a)) were more distorted than the nylon6-SFs (Figure 12(d)) after tensile testing. This implied that the interfacial adhesion via secondary bonding among PBS (polyester)-PET (polyester) was better than those of PBS (polyester)-nylon6

(polyamide). As a result, it was found that the PBS/PET-SF untreated composites had higher ultimate tensile strength than the PBS/nylon6-SF untreated composites, although the nylon6-SFs had higher tensile strength than the PET-SFs.

For HMDI or HMDA treated composites, the improved interfacial adhesion between PBS matrix and treated SFs was clearly evident by observing the fine fibrils extended from the PBS matrix to attach onto the SF surface. Considering closely with the fibrillation, the PBS matrix was able to wet the nylon6-SFs treated with HMDI (Figure 12(e)) and HMDA (Figure 12(f)) better than the PET-SFs treated. The enhancement of interfacial adhesion in the PBS/nylon6-SF composite was significantly achieved, which correlated to the shifting of tan δ to higher temperature and resulted the substantial improvement of elongation at break and impact strength

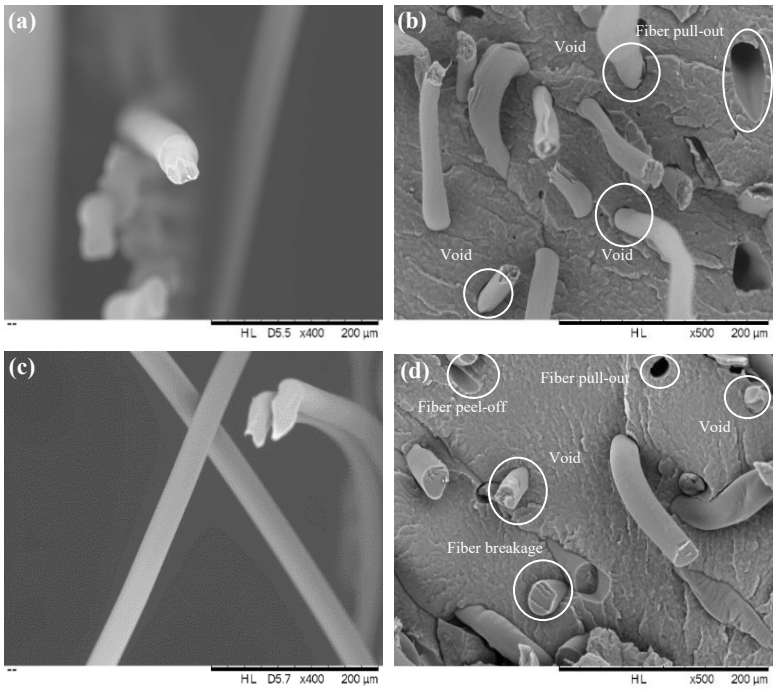

Figure 11. SEM micrographs of (a) as-received PET fibers, (b) untreated PET fibers after melt processing/cryo-fractured, (c) as-received nylon6 fibers, and (d) untreated nylon6 fibers after melt processing/cryo-fractured.

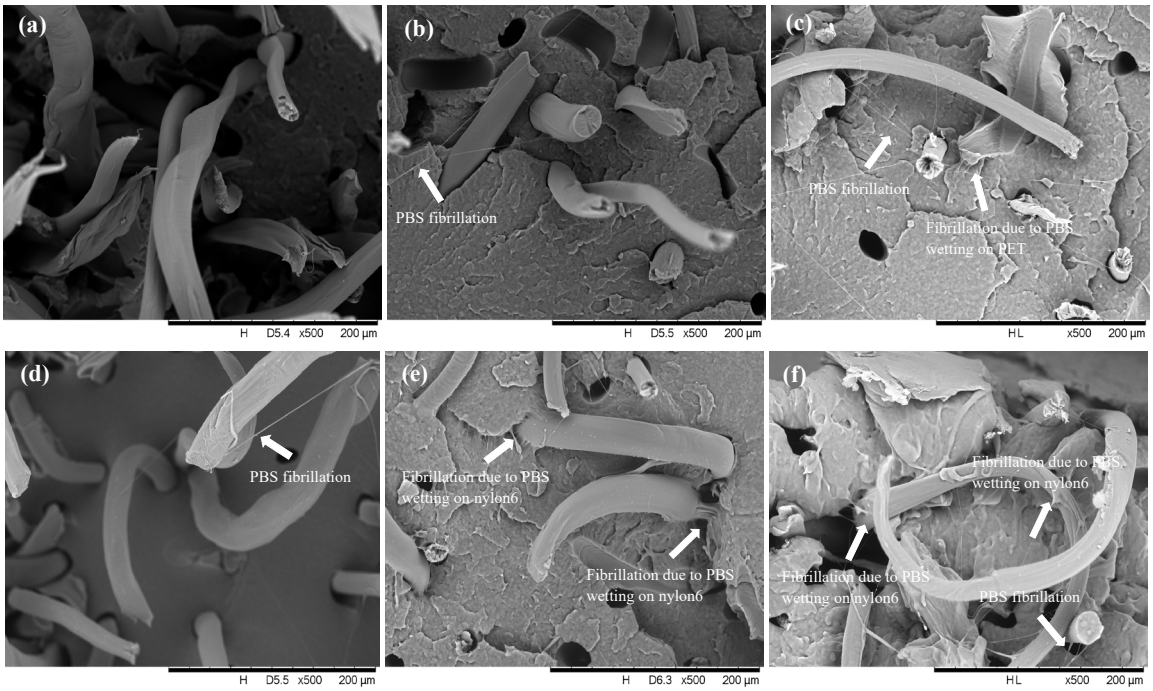

Figure 12. SEM micrographs (magnification of 500X) of tension-fractured surface of (a) PBS/PET-SF 7 wt% untreated, (b) PBS/PET-SF 7 wt% treated with HMDI, (c) PBS/PET-SF 7 wt% treated with HMDA, (d) PBS/nylon6-SF 7 wt% untreated, (e) PBS/nylon6-SF 7 wt% treated with HMDI, and (f) PBS/nylon6-SF 7 wt% treated with HMDA.

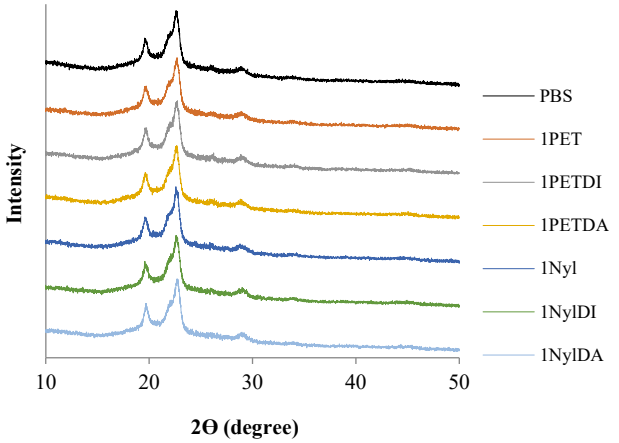

Figure 13. WXRD patterns of PBS, PBS/ untreated fiber and PBS/treated fiber composites using HMDI or HMDA.

3.6 Crystal structure of PBS matrix in the PBS/SF composites

Finally, we performed XRD studies to evaluate and compare the crystal structures of PBS and the PBS/SF composites with a fiber concentration of 1 wt%. In Figure 13, the XRD pattern of PBS shows the diffraction lines at $2\theta = 19.52°, 21.80°, 22.6°$ which are assigned to (020), (021), and (110), respectively. Qiu and Yang [30] reported the same XRD patterns for PBS. Therefore, adding these untreated or chemical treated fibers did not have alter the crystal structure of PBS, similarly to the study by Li *et al.* [7] that the PBS/Basalt composites presented the characteristic XRD peaks and there was no shift observed with the increase in Basalt fiber concentration, indicating that the crystalline structure of PBS was not affected by the addition of cellulosic fibers.

4. Conclusions

In this research study, we prepared polymer composites between PBS matrix and synthetic fibers; PET and nylon6 fibers. Two types of compatibilizers; hexamethylene diisocyanate (HMDI) or hexamethylene diamine (HMDA) of 0.05 wt% were treated on fiber surface for reactive interfacial interaction. As evident in DMA results, the shifting in T_g of PBS matrix to higher temperature indicated improved interfacial adhesion between PBS matrix and HMDA-treated fibers. The M_n of HMDI-treated composites was closed to extruded PBS; however, the M_n of HMDA-treated composites was reduced dramatically implying the occurrence of aminolysis reaction. Tensile modulus of PBS/SF composites were increased with respect to fiber concentration for untreated fibers, which PET-SFs provided better reinforcing effect. Tensile modulus of HMDA-treated composites was enhanced greater than HMDI-treated composites with the same fiber concentration. Elongation at break of both HMDI- and HMDA-treated composites was higher, and thus provided greater toughness for PBS as evident in higher notched Izod impact strength. Crystallization studies by XRD and DSC found that these chemical-treated SFs did not have impact on the PBS crystal form, while the X_c was reduced gradually due to the slower crystallization.

Acknowledgements

The authors would like to thank Department of Materials Science and Engineering, Faculty of Engineering and Industrial Technology, Silpakorn University for fully funding this research. We also appreciate Thai Toray Synthetics Co. Ltd. for kindly support PET and nylon6 fibers.

References

[1] J. H. Schut, "Waiting for Bio PBS," in *Plastics Engineering Blog* vol. 2016, ed. Worldpress.com: Society of Plastics Engineers, 2014.

[2] C. P. Hebdo, "Succinic acid: More projects for biosourced production," *Focus on Catalysts*, vol. 2009, no. 12, pp. 5-6

[3] A. A. A. Alim, A. Baharum, S. S. M. Shirajuddin, and F. H. Anuar, "Blending of low-density polyethylene and poly(butylene succinate) (LDPE/PBS) with polyethylene–graft–maleic anhydride (PE–g–MA) as a compatibilizer on the phase morphology, mechanical and thermal properties," *Polymers,* vol. 15, no. 2, pp. 261, 2023.

[4] O. Akampumuza, P. M. Wambua, A. Ahmed, W. Li, and X. Qin, "Review of the applications of biocomposites in the automotive industry," *Polymer Composites,* pp. 1-17, 2016.

[5] F. Yan-Hong, L. Yi-Jie, X. Bai-Ping, Z. Da-Wei, Q. Jin-Ping, and H. He-Zhi, "Effect of fiber morphology on rheological properties of plant fiber reinforced poly(butylene succinate) composites," *Composites Part B: Engineering,* vol. 44, no. 1, pp. 193-199, 2013.

[6] Y. Feng, H. Shen, J. Qu, B. Liu, H. He, and L. Han, "Preparation and properties of PBS/sisal-fiber composites," *Polymer Engineering & Science,* vol. 51, no. 3, pp. 474-481, 2011.

[7] L. S. Yi Li, Z. Wei, C. Ding, Y. Chang, G. Chen, W. Zhang, and J. Liang, "Mechanical properties and crystallization behavior of poly(butylene succinate) composites reinforced with basalt fiber," *Journal of Thermal Analysis and Calorimetry,* vol. 122, pp. 261-270, 2015.

[8] E. Frollini, N. Bartolucci, L. Sisti, and A. Celli, "Poly(butylene succinate) reinforced with different lignocellulosic fibers," *Industrial Crops and Products,* vol. 45, pp. 160-169, 2013.

[9] M. Zhou, Y. Li, C. He, T. Jin, K. Wang, and Q. Fu, "Interfacial crystallization enhanced interfacial interaction of poly(butylene succinate)/ramie fiber biocomposites using dopamine as a modifier," *Composites Science and Technology,* vol. 91, pp. 22-29, 2014.

[10] S. Y. Cho, M. E. Lee, H. W. Kwak, and H.-J. Jin, "Surface-modified cellulose nanocrystal-incorporated poly(butylene succinate) nanocomposites," *Fibers and Polymers,* vol. 19, pp. 1395-1402, 2018.

[11] R.-y. Chen, W. Zou, H.-c. Zhang, G.-z. Zhang, Z.-t. Yang, G. Jin, and J.-p. Qu, "Thermal behavior, dynamic mechanical properties and rheological properties of poly(butylene succinate) composites filled with nanometer calcium carbonate," *Polymer Testing,* vol. 42, pp. 160-167, 2015.

[12] J. Huang, X. Lu, N. Zhang, L. Yang, M. Yan, H. Liu, G. Zhang, and J. Qu, "Study on the properties of nano-TiO_2/ polybutylene succinate composites prepared by vane extruder," *Polymer Composites,* vol. 35, no. 1, pp. 53-59, 2014.

[13] F. B. Ali, and R. Mohan, "Thermal, mechanical, and rheological properties of biodegradable polybutylene succinate/carbon nanotubes nanocomposites," *Polymer Composites,* vol. 31, no. 8, pp. 1309-1314, 2010.

[14] A. K. Maurya, S. Kumar, M. Singh, and G. Manik, "Polyamide fiber reinforced polymeric composites: A short review," *Volume 80, Part 1,* vol. 80, no. 1, pp. 98-103, 2023.

[15] T. N. Abraham, and K. E. George, "Studies on recyclable nylon-reinforced PP composites: Effect of fiber diameter," *Journal of Thermoplastic Composite Materials,* vol. 22, no. 1, pp. 5-20, 2009.

[16] F. Ke, X. Jiang, H. Xu, J. Ji, and Y. Su, "Ternary nano-$CaCO_3$/ poly(ethylene terephthalate) fiber/polypropylene composites: Increased impact strength and reinforcing mechanism," *Composites Science and Technology,* vol. 72, no. 5, pp. 574-579, 2012.

[17] S.-H. Lee and S. Wang, "Biodegradable polymers/bamboo fiber biocomposite with bio-based coupling agent," *Composites: Part A,* vol. 37, pp. 80-91, 2006.

[18] G. N. Onyeagoro, E. G. Ohaeri, I. O. Arukalam, M. J. Uko, U. O. Enwereuzoh, and C. O. Uzoig, "Effects of MAPI/HMDA dual compatibilizer and filler loading on physico-mechanical and water sorption properties of natural rubber/poly (ethylene terephthalate) (PET)/dikanut shell powder bio-composites," *British Journal of Applied Science & Technology,* vol. 4, no. 23, pp. 3383-3401, 2014.

[19] N. Hongsriphan, W. Muangrak, K. Soonthornvacharin, and T. Tulaphol, "Mechanical improvement of poly(butylene succinate) with polyamide short fibers," *Macromolecular Symposia,* vol. 354, pp. 28-34, 2015.

[20] Y. J. Phua, N. S. Lau, K. Sudesh, W. S. Chow, and Z. A. M. Ishak, "Biodegradability studies of poly(butylene succinate)/ organo-montmorillonite nanocomposites under controlled compost soil conditions: Effects of clay loading and compatibiliser," *Polymer Degradation and Stability,* vol. 97, pp. 1345–1354, 2012.

[21] T.-x. Jin, M. Zhou, S.-d. Hu, F. Chen, and Q. Fu, "Effect of molecular weight on the properties of poly(butylene succinate)," *Chinese Journal of Polymer Science,* vol. 32, no. 7, pp. 953-960, 2014.

[22] M. Asgari and M. Masoomi, "Tensile and flexural properties of polypropylene/short poly(ethylene terephthalate) fibre composites compatibilized with glycidyl methacrylate and maleic anhydride," *Journal of Thermoplastic Composite Materials* vol. 28, no. 3, pp. 357-371, 2015.

[23] B. Tan, J.-p. Qu, L.-m. Liu, Y.-h. Feng, S.-x. Hu, and X.-c. Yin, "Non-isothermal crystallization kinetics and dynamic mechanical thermal properties of poly(butylene succinate) composites reinforced with cotton stalk bast fibers," *Thermochimica Acta,* vol. 525, pp. 141-149, 2011.

[24] P. Liminana, D. Garcia-Sanoguera, L. Quiles-Carrillo, R. Balart, and N. Montanes, "Development and characterization of environmentally friendly composites from poly(butylene succinate) (PBS) and almond shell flour with different compatibilizers," *Composites Part B: Engineering,* vol. 144, pp. 153-162, 2018.

[25] P. Rizzarelli and S. Carroccio, "Thermo-oxidative processes in biodegradable poly(butylene succinate)," *Polymer Degradation and Stability,* vol. 94, pp. 1825-1838, 2009.

[26] P. Raffa, M.-B. Coltelli, S. Savi, S. Bianchi, and V. Castelvetro, "Chain extension and branching of poly(ethylene terephthalate) (PET) with di- and multifunctional epoxy or isocyanate additives: An experimental and modelling study," *Reactive & Functional Polymers,* vol. 72, pp. 50-60, 2012.

[27] H. Zahn and H. Pfeifer, "Aminolysis of polyethylene terephthalate," *Polymer,* vol. 4, pp. 429-432, 1963.

[28] A. M. Al-Sabagh, F. Z. Yehia, G. Eshaq, A. M. Rabie, and A. E. ElMetwally, "Greener routes for recycling of polyethylene terephthalate," *Egyptian Journal of Petroleum,* vol. 25, no. 1, pp. 53-64, 2016.

[29] R. M. Musale and S. R. Shukla, "Deep eutectic solvent as effective catalyst for aminolysis of polyethylene terephthalate (PET) waste," *International Journal of plastic technology,* vol. 20, no. 1, pp. 106-120, 2016.

[30] Z. Qiu and W. Yang, "Crystallization kinetics and morphology of poly(butylene succinate)/poly(vinyl phenol) blend," *Polymer,* vol. 47, pp. 6429-6437, 2006.